Stresses in Soils due to Axially Loaded Friction Pile

by

N. Roy*
V. Singh**

Introduction

Estimation of the vertical stress distribution in soils due to vertical load is largely based on the work of Boussinesq (1885) and Mindlin (1936). Assuming that the vertical load is transferred to the soil as line load through the axis of the pile, Geddes (1966, 69) obtained stress coefficients for various distribution (vertical) of the line load. Since the radial dimension of the pile was neglected in this analysis, Geddes' stress coefficients for location in the neighbourhood of the pile are obviously in error. Singh (1972) sought to remove this defect by taking into account both the pile-length and the pile diameter. However, the stress coefficients obtained by Singh are also approximate, especially in the pile shaft, as the discontinuity in the soil medium in the space occupied by the pile was not accounted for in this analysis.

In the present investigation the stress-coefficients have been obtained for vertically loaded friction piles on the assumption that the pile load is transferred to the soil as a uniform shearing stress along the periphery of the pile shaft. The analysis takes into account both the pile length and the pile diameter and neglects the radial stress produced at the pile-shaft by the shaft loading. The use of the stress coefficients in the estimate of the settlement of pile group has been demonstrated by working out an example.

Method of Analysis

Figure 1 (*a*) represents an outline of a cylindrical pile of length L and radius embedded in a homogeneous, isotropic, elastic half space defined by G and μ. The analysis is essentially to find a system of fictitious vertical point loads P_j, $j = 1, \ldots\ldots, N$ which, when applied at the axis of the pile at varying depths (see Figure 1 (*b*)) produce stresses at the pile shaft soil interface identical to those created by the axially loaded friction pile and at the same time satisfy the stress boundary conditions on the free surface of the half space. The discrete vertical point loads P_j are fictitious in that they are to be applied along the real pile axis to produce identical stress conditions in the half space figure and do not necessarily add up to the vertical load P_o acting on the real pile. However, once the P_j values have been determined it is a simple matter to calculate the actual stresses and displacements they produce any where in the half space including those on the real pile boundaries.

*Professor of Civil Engineering, Institute of Technology, B.H.U.
**Lecturer in Civil Engineering, Institute of Technology, B.H.U. Varanasi-5 India.
The paper is open for discussion till August 1975.

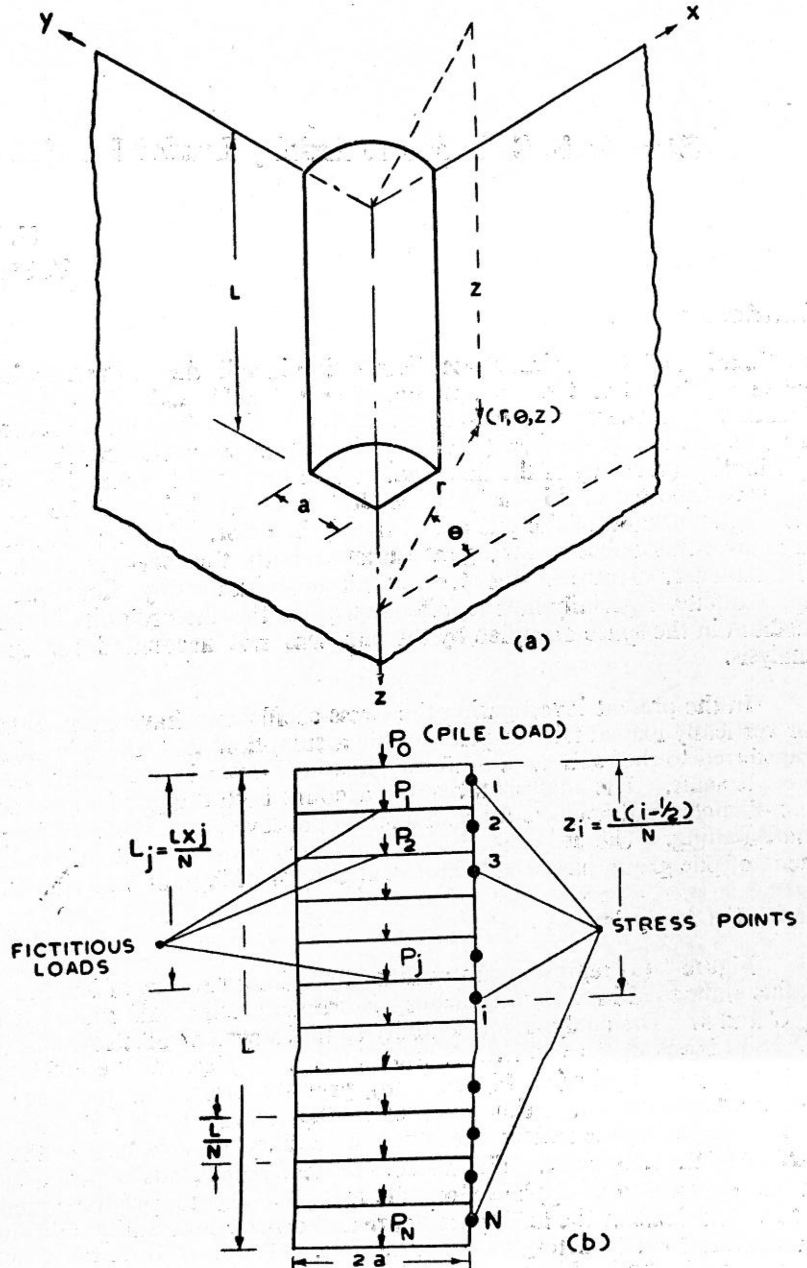

FIGURE 1. *(a)* **Quadrant of Elastic Half-Space with Pile (radius=a, length=L Removed; *(b)* System Fictitious Loads and Stress Points**

Determination of the Fictitious Load System

A vertically loaded pile induces vertical, radial, circumferential and shearing stresses at all points including those at the pile-shaft medium interface. Since a friction pile is one which transfers its loads entirely by skin friction, the shear stresses induced at the interfacial boundary of the elastic medium must be in equilibrium with the pile load. In the present analysis the vertical distribution of this pile induced shear stress at the pile shaft medium interface is assumed uniform over the length of the pile, although the method of analysis adopted can easily be extended to cover any arbitrary distribution of this loading.

Figure 1 (*b*) shows the distribution of the fictitious vertical point load P_j at the real pile axis as well as the location of the "Stress points" at the pile shaft-medium interface at which the induced shear stresses are matched with the pile skin friction. Using the Mindlin solution for a vertical point load applied below the surface of the elastic half space, the total shear stress induced by the set of fictitious loads at a stress point i ($r = a$, $z = z_i$) can be written as

$$T_i = \sum_{j=1}^{N} E_{ij} P_j, \; i = 1, \ldots N \qquad \ldots(1)$$

where the coefficients E_{ij} are easily obtainable from the Mindlin (1936) solution.

It P_o is the real pile load and the boundary shear stresses are assumed uniform,

$$T_i = \frac{P_o}{2\pi aL} \qquad \ldots(2)$$

Substitution of Equation (2) in Equation (1) gives

$$\sum_{j=1}^{N} E_{ij} P_j = \frac{P_o}{2\pi aL}, \; i = 1, \ldots N \qquad \ldots(3)$$

Dividing both sides of Equation (3) by $\frac{P_o}{2\pi aL}$ and replacing P_j/P_o by the non-dimensionalised set of fictitious loads P_j, $j = 1, \ldots N$, the following matrix equation is obtained.

$$[C]\,(p) = (U) \qquad \ldots(4)$$

It can be shown directly from the Geddes, 'non-dimensionalised presentation of the Mindlin equations and with reference to Figure 1 (*b*) that the elements C_{ij} of the $N \times N$ coefficient matrix $[C]$ in Equation (4) are given by

$$C_{ij} = \frac{N^3}{j^3}\left(\frac{a}{L}\right)^2 \frac{1}{4(1-\mu)} \left[-\frac{(1-2\mu)}{A^3_{ij}} + \frac{(1-2\mu)}{B^3_{ij}} - \frac{3(m_o-1)^2}{A^5_{ij}}\right.$$

$$-\left\{\frac{3\,(3-4\,\mu)m_o\,(m_o+1)-3\,(3m_o+1)}{B^5_{ij}}\right\}-\frac{30m_o\,(m_o+1)^2}{B^7_{ij}}\Bigg]\ldots(5)$$

Where, $A_{ij}=\left\{n^2_o+(m_o-1)^2\right\}^{1/2}$

$$B_{ij}=\left\{n^2_o+(m_o+1)^2\right\}^{1/2}$$

$$n_o=\frac{a}{L}\cdot\frac{N}{j}$$

$$m_o=\frac{(i-1/2)}{j}$$

Also, the elements u_i of the N dimensional constant vector (U) are all unity. Solution of the matrix Equation (4) gives the non-dimensional fictitious load vector as

$$(p)=[C^{-1}]\,(U)=[B]\,(U)$$

since all the elements of (U) are unity

$$p_j=\sum_{j=1}^{N}B_{ij};\ i=1,\ldots.,N \qquad \ldots(6)$$

Determination of the Vertical Stress Coefficients

The set of fictitious loads with magnitude given by Equation (6) and points of application defined by Figure 1 (b) replaces the pile load P_o for all calculations of pile load stresses in the elastic half space. The pile induced vertical stress σ_{zz} at a point in the medium therefore equals the sum of the vertical stresses induced at that point by each of the above fictitious loads individually. Defining the vertical stress coefficients $K_{zz}=\sigma_{zz}\times L^2/P_o$, an expression for the same can be written as

$$K_{zz}=\sum_{j=1}^{N}F_j\,p_j \qquad \ldots(7)$$

where the coefficients F_j derived from the Mindlin equation for the non-dimensional co-ordinate location m,n for the fictitious axial loads p_j are to be evaluated from the following expression

$$F_j=\frac{N^2}{j^2}\;\frac{1}{8\pi\,(1-\mu)}\Bigg[-\frac{(1-2\,\mu)\,(m_j-1)}{A_j^3}+\frac{(1-2\mu)\,(m_j-1)}{B_j^3}-\frac{3(m_j-1)^3}{A_j^5}$$
$$-\left\{\frac{3\,(3-4\,\mu)\,m_j\,(m_j+1)^2-3\,(m_j+1)\,(5m_j-1)}{B_j^5}\right\}-\frac{30m_j\,(m_j+1)^3}{B_j^7}\Bigg] \qquad \ldots(8)$$

where,

$$A_j=[n_j^2+(m_j-1)^2]^{1/2}$$
$$B_j=[n_j^2+(m_j+1)^2]^{1/2}$$

$$n_j = \frac{r}{L} \cdot \frac{N}{j}$$

$$m_j = \frac{z}{L} \cdot \frac{N}{j}$$

Equations (6) and (7) were programmed for solution in an IBM 7044 digital computer. A large number of trial computations were run for selecting an optimum value of N. All results reported here were computed with $N = L/a$ for which both convergence and stability were found to be satisfactory.

Results

Vertical stress coefficients have been obtained for a wide range of value of m, n, μ and L/a. Tables (1—9) give the stress coefficients for three values of poisson's ratio ($\mu = 0.1, 0.3$ and 0.5) and for three values of length-radius ratio ($L/a = 40, 60$ and 120). Above parameters have been chosen because the majority of the field problems involving friction piles come within these limits. In view of the equation involved, it is considered that tabulated values of stress-coefficients are of greater use in practice.

In order to demonstrate the influence of pile dimensions on the stress coefficients, a limited comparison of the tabulated results with those due to Geddes (who neglected the pile radius completely in his analysis) has been presented graphically in Figure 2 and Figure 3. In these figures, the stress coefficients for the shortest ($L/a = 40$) and the longest ($L/a = 120$) of the three piles have been compared with those of the Gedde's pile ($L/a = \infty$). Figures 2(a) and 2(b) show this comparison for $\mu = 0.1$ and $\mu = 0.5$ respectively, on a horizontal plane passing slightly below the pile tip ($m = 1.1$). Similarly, Figures 3(a) and 3(b) compare the distribution of the vertical stress coefficients along the pile axis ($n = 0$).

Application of the results in settlement analysis

The use of the tables is illustrated by the following example.

Problem

A pile group consists of 4 circular piles, each of 12m embedded length. The piles are assumed to transfer their loads, entirely by skin friction, to a normally consolidated soft clay having a saturated unit wt. $\gamma = 1.72$ gram/cm^3, a void ratio $e = 1.0$ and a poisson's ratio $\mu = 0.30$. The pile cap, of size $4d \times 4d$, where d is the pile diameter carries a central vertical load of 100 tonnes so that the each friction pile is subjected to an axial load of $P_o = 25$ tonnes. Using Tables 2, 5 and 8 estimate the settlement of the quarter points of the pile-cap (see Figure 4) for L/d ratio of 20, 30 and 60 and compare the results with those obtained from Geddes tables and from the conventional method. Assume C_c for the soil $= 0.3$.

Solution

The vertical settlement ρ of a surface point, due to consolidation of the underlying horizontal layers in which the semi-infinite subsurface zone may be assumed to be divided, is given by

$$\rho = \frac{0.4343\, C_c}{1+e} \Sigma \triangle h \log_e \left(1 + \frac{\Delta\sigma_1}{\sigma_1}\right)$$

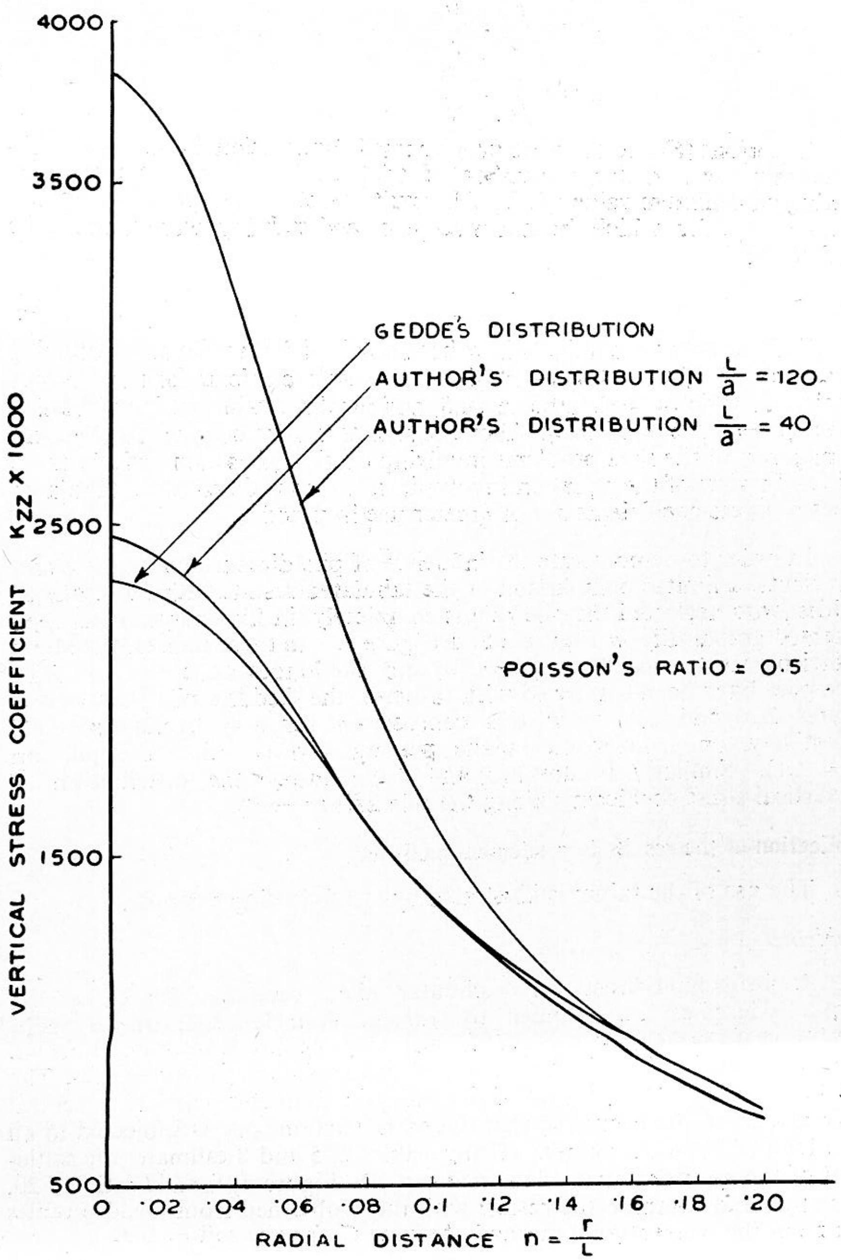

FIGURE 2(*a*) Distribution of Vertical Stress Coefficient on Horizontal Plane (m=1.1, μ = 0.5)

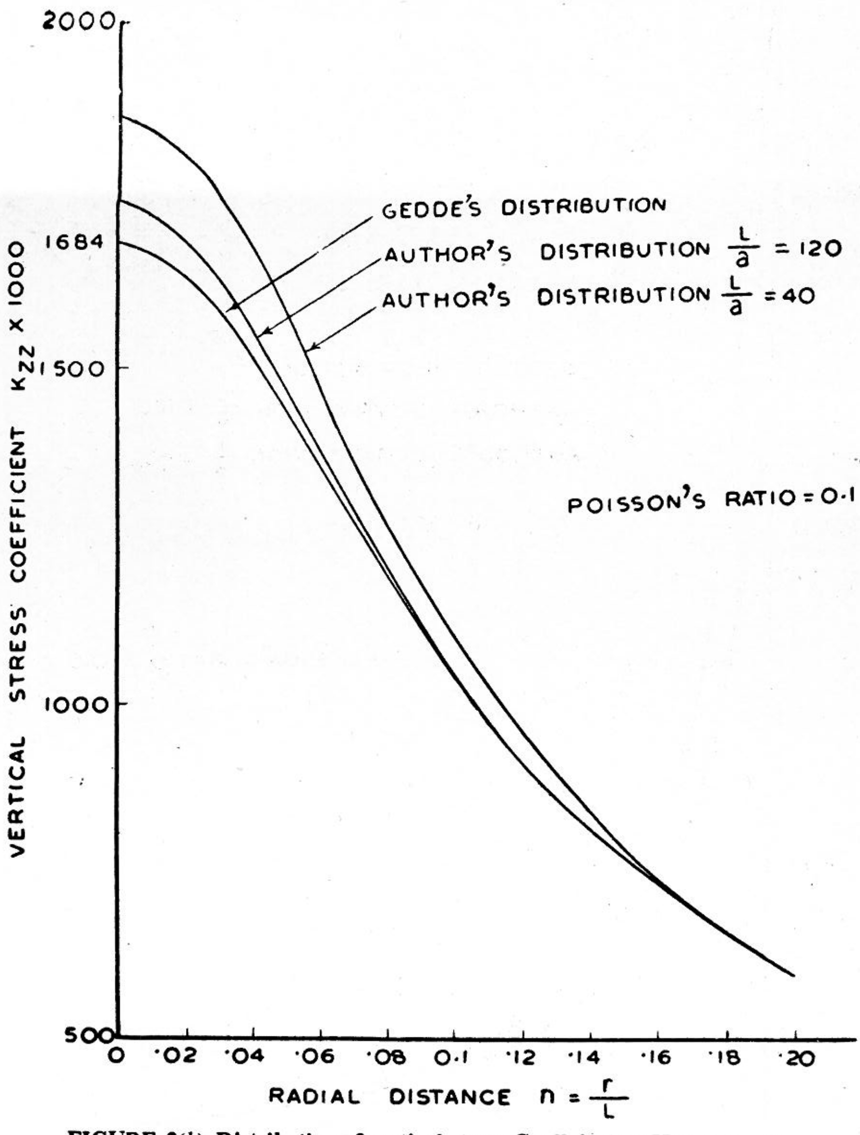

FIGURE 2(*b*) Distribution of vertical stress Coefficient on Horizontal Plane ($m = 1.1$, $\mu = 0.1$)

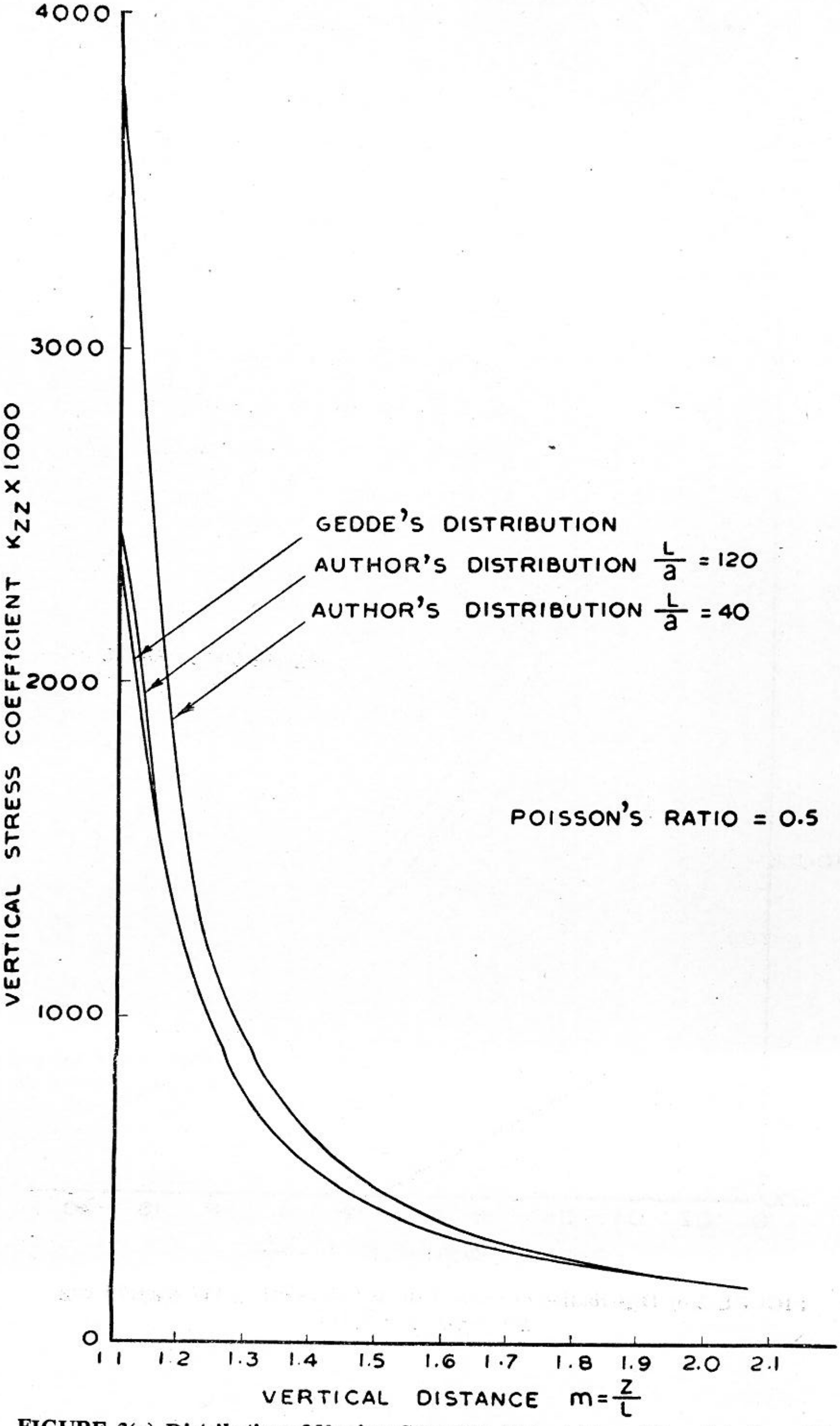

FIGURE 3(*a*) **Distribution of Vertical Stress Coefficient Along Line of Action of Load ($n = 0$, $\mu = 0.5$)**

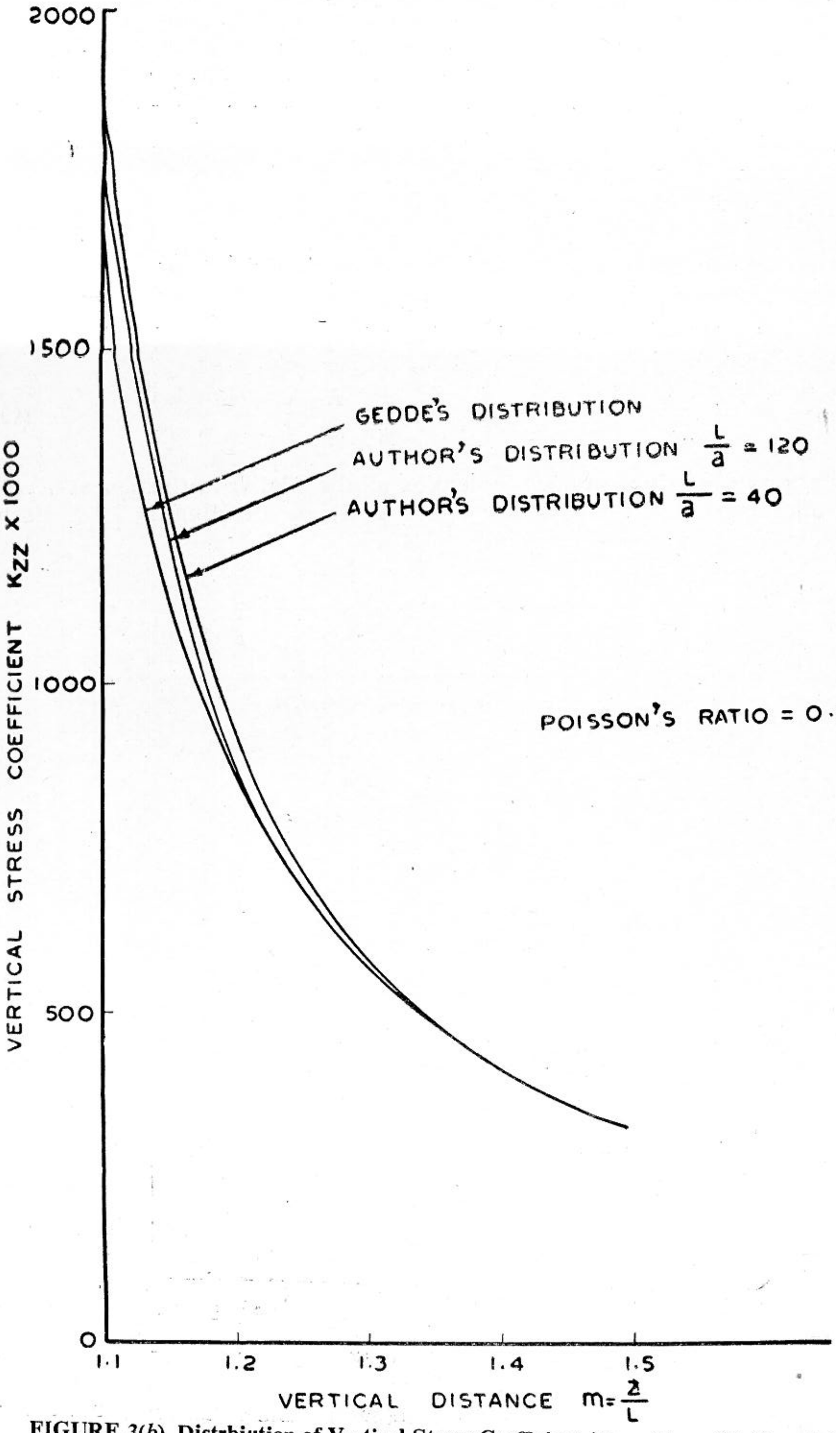

FIGURE 3(b) Distrbiution of Vertical Stress Coefficient Along Line of Action of Load ($n = 0; \mu = 0.1$)

where, $\triangle h$ is the layer thickness, σ_1 is the initial intergranular stress at mid-depth of the layer at a point vertically below the surface point, and $\triangle \sigma_1$ is the vertical stress increment at the same point due to transfer of pile-loads. If it is assumed that the initial inter granular stress is due to only over-burden pressure, the above equation can be written in the following non-dimensional form

$$\rho/L = \frac{.4343\ C_c}{1+e} \Sigma\ \delta \log_e \left(1 + \frac{K_{zz}}{m} \frac{P}{\gamma L^3}\right)$$

where, δ is the non-dimensional layer thickness $= \triangle h/L$, and K_{zz} is the vertical stress coefficient $= \sigma_{zz} \times L^2/P$. Substitution of the numerical values of the soil constants, the pile load, the pile length, results in the following simplified equation

$$\rho/L = 0.065\ \delta \log_e \left(1+0.0084\ \frac{K_{zz}}{m}\right) \qquad ...(9)$$

Equation (9) has been applied to determine the relative settlement (ρ/L) of the quarter point of the pile cap (see Figure 4) by dividing a 2.7 L deep

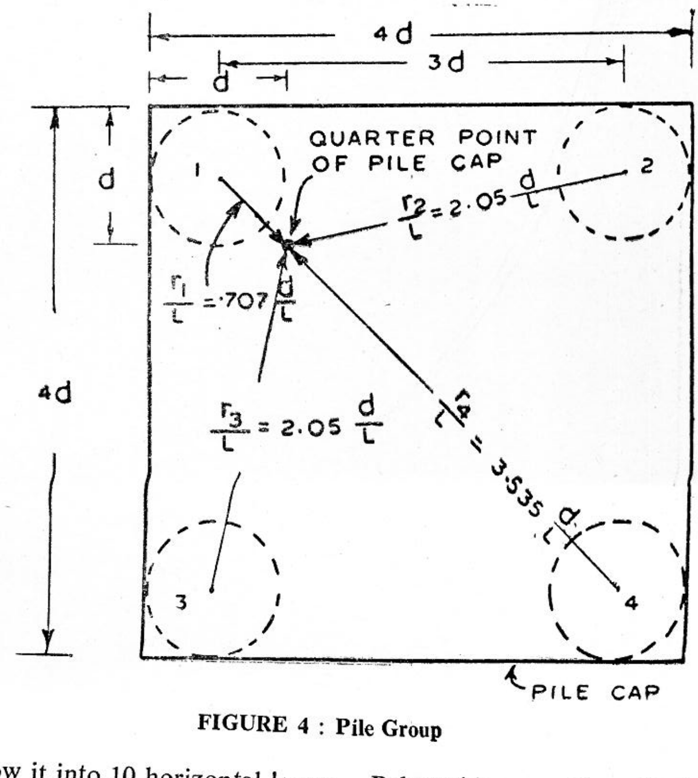

FIGURE 4 : Pile Group

zone below it into 10 horizontal layers. Below this zone the pile induced vertical stresses are very small and the resultant settlement is negligible. Table (10) shows typical calculations using appropriate values of the coefficients K_{zz} from Table (5) for the case $L/d = 30$ and $\mu = 0.3$. Result of

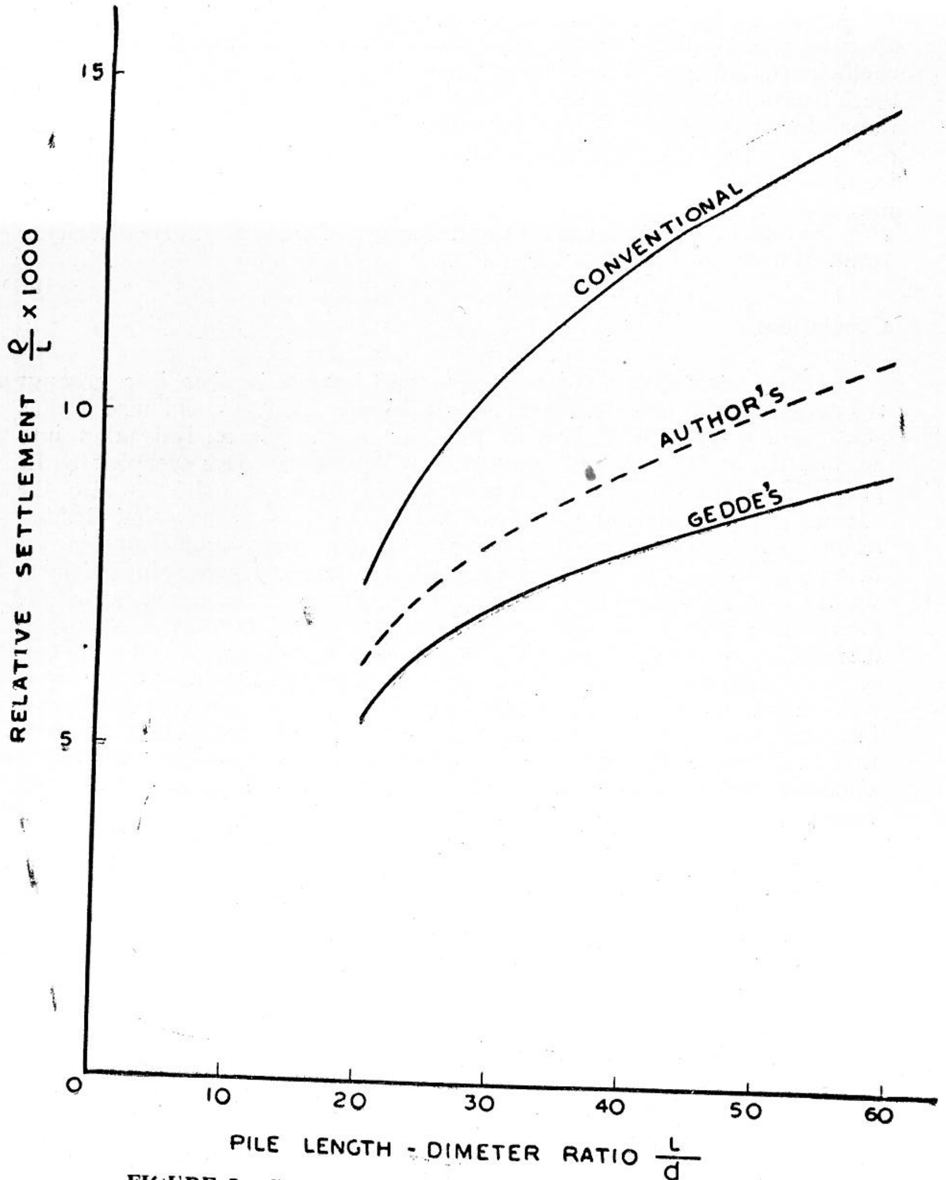

FIGURE 5 : Settlement of a 4—Pile Group—Varying *L*/*d* Ratio

this and similar estimates for $L/d = 20$ and 60 are compared graphically in Figure 5 with those calculated from (*i*) Geddes' stress coefficients and (*ii*) conventional method.

Examination of Figure 5 shows that the settlement estimates based on the present analysis are higher than those predicted from Geddes' stress coefficients. However, the difference between the two estimates decreases as the L/d ratio is reduced. This is because with increasing L/d the relative radial distances r/L of the quarter point of the pile cap from the closest pile increases and the difference between the induced stresses obtained from the present and Geddes' data reduces [See Figures 2 (*a*) and 2 (*b*)]. It may also be noted that in all the cases the conventional method considerably over-estimates the settlement and that use of Geddes' stress coefficients result in nonconservative estimates.

Conclusions

The present investigation is more exact because it takes into account the actual mechanism of load transfer from pile shaft to soil medium as shear load along the periphery of the pile shaft. The analysis takes into account the discontinuity in the elastic medium in the space occupied by the pile. The graphical comparison presented in Figures 2 and 3 as also the comparison of tabulated results with those due to Geddes' show that Geddes' results give conservative values for the vertical stress-coefficients in the neighbourhood of pile shaft, a zone which is of primary interest in settlement studies. For large values of L/a ratio, the influence of pile-radius is smaller and the results of the present analysis agree with those of Geddes' much nearer the pile. In fact, as $L/a \rightarrow \infty$ Geddes' solution is obtained as a limiting case of the present analysis. Settlement analysis carried out for a 4-pile group of friction piles show that the estimates based on the stress coefficients obtained in the present study are much lower than those obtained from the conventional method of analysis. But the same settlements are higher than those obtained from Geddes' stress coefficients, the difference increasing with increasing L/d.

Notation

a radius of friction pile

d diameter of friction pile

L length of friction pile

P_o axial load of friction pile

μ poisson's ratio

G shear Modulus

N number of equally spaced fictitious axial loads P_j as also number of equally spaced 'stress points'.

i serial number of stress points at which shear stress induced by the fictitious axial loads are matched with real pile skin friction.

j serial number of the fictitious load P_j

P_j fictitious load applied at the real pile axis.

p_j non-dimensionalised fictitious load P_j/P_o

(p) n-dimensional column vector with elements p_j

r, z radial and vertical coordinates in the cylindrical coordinate system, of a point in the elastic half space.

m, n non-dimensionalised vertical and radial coordinates of a point in the elastic half space defined as $m = z/L$, $n = r/L$.

m_j, n_j non-dimensionalised vertical and radial coordinates, of a point in the elastic half space for the j th pile.

m_o, n_o non-dimensionalised vertical and radial coordinates of the i th point on the pile shaft for the j th pile.

$[C]$ $N \times N$ coefficient matrix

$[B]$ inverse matrix of the matrix $[C]$

T_i shear stress induced at point $(r = a, z = z_i)$

σ_{zz} Vertical stress induced at point (r, z)

K_{zz} vertical stress coefficient defined as $\sigma_{zz} \times L^2/P_o$ for the point (m, n)

F_j contribution of the load p_j in the vertical stress coefficient K_{zz} at the point (m, n) of the elastic half space.

References

APPOLONIA, D. and ROMOALDI, J.P. (1963). 'Load transfer in End Bearing Steel, H. Piles.' *Proc. Am. Soc. Civ. Engg.*, 89, SM 2.1.

BOUSSINESQ, J. (1885). 'Application of Potential to the Study of the Equilibrium and Movements in Elastic soils'. *Gauthier-Villard*, Paris.

BUTTERFIELD, R. and BANERJEE, P.K. (1971*a*). 'The elastic analysis of compressible piles and pile groups'. *Geotechnique* 21, No. 1, pp. 43-60.

GEDDES, J.D. (1966). 'Stresses in foundation soils, due to vertical subsurface loading. *Geotechnique Volume* 21, No. 3, pp. 231-265.

GEDDES, J.D. (1969). 'Boussinesq based approximation to the vertical stresses caused by pile-type-subsurface loading' *Geotechnique* 19, No. 4, pp. 509-514.

MINDLIN, R.D. (1936). 'Force at a point in the interior of a semi-infinite solid'. Physics 7, 195-200.

SINGH, VIRENDRA (1972). 'Stress coefficients in soils due to vertical load on single pile of varying length-diameter ratio'. *Modern trend in Civil Engineering*, Roorkee, November 11-13.

Appendix I

Table 1: Values of $K_{zz} \times 1000$ for uniform skin friction for $\mu = 0.1$ and $L/a = 40.0$
(+Tension, otherwise compression)

m \ n	0.0	0.025	0.04	0.06	0.08	0.1	0.12	0.16	0.2	0.4	0.8	1.0	2.0	2.5	3.0
0.1	0.0	1211	1232	984	743	551	408	233	142	26	4	2	0	0	0
0.3	0.0	538	534	521	502	479	452	395	337	140	29	14	1	0	0
0.5	0.0	441	440	436	431	423	413	390	363	218	61	32	2	1	0
0.7	0.0	515	549	543	535	523	509	477	440	266	87	50	4	2	1
0.9	0.0	1279	1188	1139	1054	956	863	704	584	290	103	63	7	3	1
1.0	0.0	7244	3309	2050	1539	1232	1025	767	612	291	107	68	8	3	2
1.1	1867	1778	1657	1459	1261	1087	943	732	592	287	110	72	10	4	2
1.3	573	570	534	554	540	524	505	465	423	239	112	76	13	6	3
1.5	325	325	324	321	318	314	310	299	286	213	108	77	15	7	4
1.7	221	221	220	219	218	217	215	211	205	170	100	75	18	9	5
1.9	163	163	163	163	162	161	161	158	156	136	90	71	19	10	6
2.1	127	127	127	127	126	126	126	124	123	111	80	65	21	11	6
2.3	102	102	102	102	102	102	102	101	100	93	71	60	21	12	7
2.5	85	85	85	85	84	84	84	84	83	78	63	54	22	13	8
2.7	71	71	71	71	71	71	71	71	70	67	55	49	21	14	9
3.0	57	57	57	57	57	56	56	56	56	54	48	42	21	14	9

TABLE 2: Values of $K_{zz} \times 1000$ for uniform skin friction for $\mu=0.3$ and $L/a=40.0$
(+Tension, otherwise compression)

m \ n	0.0	0.025	0.04	0.06	0.08	0.1	0.12	0.16	0.2	0.4	0.8	1.0	2.0	2.5	3.0
0.1	0.0	4720	820	699	663	527	400	231	142	26	4	2	0	0	0
0.3	0.0	2908	289	344	457	469	450	359	339	142	29	14	0	0	0
0.5	0.0	1329	365	386	428	433	426	402	374	224	61	32	2	0	0
0.7	0.0	+195	665	637	585	561	543	507	466	276	87	49	4	1	0
0.9	0.0	+995	1530	1405	1185	1046	936	575	624	301	103	62	6	2	1
1.0	0.0	8015	3592	2162	1629	1312	1094	816	648	302	107	67	8	3	1
1.1	2177	2064	1910	1664	1421	1210	1039	794	635	299	111	71	9	4	2
1.3	646	642	635	623	606	586	564	516	466	275	114	76	12	5	2
1.5	361	361	359	357	353	348	343	330	314	229	111	78	15	7	3
1.7	243	343	242	241	240	238	236	231	225	183	104	77	17	8	4
1.9	178	178	178	177	177	176	175	172	169	147	95	73	19	10	5
2.1	138	138	138	137	137	137	136	135	133	120	84	68	20	11	6
2.3	111	110	110	110	110	110	109	109	107	99	75	62	21	12	7
2.5	91	91	91	91	91	90	90	90	89	83	66	56	22	13	8
2.7	76	76	76	76	76	76	76	75	75	71	58	51	22	13	8
3.0	60	60	60	60	60	60	60	60	59	57	49	44	21	14	9

TABLE 3: Values of $K_{zz} \times 1000$ for uniform skin friction for $\mu=0.5$ and $L/a=40.0$
(+Tension, otherwise compression)

m \ n	0.0	0.025	0.04	0.06	0.08	0.1	0.12	0.16	0.2	0.4	0.8	1.0	2.0	2.5	3.0
0.1	0.0	+2803	838	1056	753	537	401	241	151	27	4	2	0	0	0
0.3	0.0	+987	476	607	528	472	436	380	330	145	29	14	0	0	0
0.5	0.0	1306	460	376	407	422	421	403	377	230	62	32	1	0	0
0.7	0.0	3741	627	324	452	520	538	519	482	290	89	48	3	1	0
0.9	0.0	6452	1225	696	876	945	925	800	673	321	104	61	5	1	0
1.0	0.0	7757	2294	1835	1682	1442	1220	907	714	322	109	66	6	2	1
1.1	3839	3502	3078	2467	1943	1549	1268	917	715	321	113	71	7	3	1
1.3	877	870	858	836	807	773	735	655	578	311	119	78	10	4	2
1 5	460	459	457	453	447	440	431	411	388	267	120	82	13	6	2
1.7	300	299	299	297	295	293	290	282	273	216	115	82	16	7	3
1.9	216	215	215	214	213	212	211	207	203	173	105	78	18	9	4
2.1	164	164	164	164	163	163	162	160	158	140	95	75	20	10	5
2.3	160	130	130	130	130	129	129	128	126	115	84	69	21	12	6
2.5	106	106	106	106	106	105	105	104	104	96	75	63	22	13	7
2.7	88	88	88	88	88	88	88	87	87	82	66	57	22	13	8
3.0	69	69	69	69	69	69	69	69	68	65	55	49	22	14	9

TABLE 4: Values of $K_{zz} \times 1000$ for uniform skin friction for $\mu = 0.1$ and $L/a = 50.0$
(+Tension, otherwise compression)

m \ n	0.0	0.02	0.04	0.06	0.08	0.1	0.12	0.16	0.2	0.4	0.8	1.0	2.0	2.5	3.0
0.1	0.0	1369	1208	963	732	546	407	234	143	26	4	2	0	0	0
0.3	0.0	550	542	328	508	484	456	396	339	140	28	14	1	0	0
0.5	0.0	451	449	444	437	429	419	395	367	219	61	32	2	1	0
0.7	0.0	570	567	560	549	536	520	485	446	267	87	50	4	2	1
0.9	0.0	1340	1294	1203	1091	979	876	708	586	290	103	63	7	3	1
1.0	0.0	7877	3070	2049	1534	1226	1021	764	610	291	107	68	8	3	2
1.1	1820	1761	1609	1416	1226	1060	923	722	586	286	110	72	10	4	2
1.3	562	560	554	554	531	515	497	558	418	257	111	76	13	6	3
1.5	321	321	319	317	314	310	306	295	282	211	107	77	15	7	4
1.7	218	218	218	217	216	214	213	208	203	168	99	75	18	9	5
1.9	162	162	161	161	161	160	159	157	154	135	90	70	19	10	6
2.1	126	126	126	126	125	125	125	123	122	111	80	65	20	11	6
2.3	102	102	102	101	101	101	101	100	99	92	70	59	21	12	7
2.5	84	84	84	84	84	84	83	83	82	77	62	54	21	13	8
2.7	71	71	71	71	71	70	70	70	70	66	55	48	21	13	8
3.0	56	56	56	56	56	56	56	56	56	53	46	42	21	14	9

TABLE 5: Values of $K_{zz} \times 1000$ for uniform skin friction for $\mu = 0.3$ and $L/a = 60.0$
(+Tension, otherwise compression)

m \ n	0.0	0.02	0.04	0.06	0.08	0.1	0.12	0.16	0.2	0.4	0.8	1.0	2.0	2.5	3.0
0.1	0.0		3139	1239	784	561	411	233	142	26	4	2	0	0	0
0.3	0.0		+656	408	513	499	471	410	350	144	28	13	0	0	0
0.5	0.0		608	488	467	457	446	420	389	228	61	31	2	0	0
0.7	0.0		1643	741	624	599	579	535	487	280	66	48	3	1	0
0.9	0.0		+178	1244	1268	1129	994	782	636	301	102	61	6	2	1
1.0	0.0		3891	2202	1646	1317	1094	815	647	301	106	66	7	3	1
1.1	1721		1582	1435	1272	1117	980	769	623	297	110	70	9	3	2
1.3	593		585	575	561	545	527	486	444	269	112	75	12	5	2
1.5	342		340	338	335	330	326	314	300	222	110	77	14	7	3
1.7	233		232	231	230	228	226	222	216	178	102	76	17	8	4
1.9	172		171	171	170	170	169	166	164	143	93	72	18	9	5
2.1	133		133	133	133	132	132	130	129	116	82	67	20	11	6
2.3	107		107	107	107	106	106	105	104	96	73	61	21	12	7
2.5	88		88	88	88	88	88	87	86	81	64	55	21	13	7
2.7	74		74	74	74	74	74	73	37	69	57	50	21	13	8
3.0	59		59	59	59	59	58	58	58	56	48	43	21	14	9

TABLE 6: Values of $K_{zz} \times 1000$ for uniform skin friction for $\mu = 0.5$ and $L/a = 60.0$
(+Tension, otherwise compression)

m \ n	0.0	0.02	0.04	0.06	0.08	0.1	0.12	0.16	0.2	0.4	0.8	1.0	2.0	2.5	3.0
0.1	0.0	3667	632	748	659	517	495	232	144	27	4	2	0	0	0
0.3	0.0	1959	273	442	486	477	454	399	343	146	29	13	0	0	0
0.5	0.0	709	441	465	468	462	451	426	396	235	61	31	1	0	0
0.7	0.0	+336	838	702	646	621	601	558	511	294	87	47	2	1	0
0.9	0.0	+598	1859	1506	1301	1162	1041	841	689	320	102	60	5	1	0
1.0	0.0	7312	3272	2417	1847	1473	1219	902	711	320	108	65	6	2	1
1.1	3058	2906	2533	2104	1724	1426	1200	896	707	320	112	70	7	2	1
1.3	793	789	778	760	737	709	678	611	545	304	117	76	10	4	2
1.5	430	430	427	424	419	413	405	388	367	358	117	80	13	5	2
1.7	284	284	283	282	280	278	275	268	260	208	112	80	16	7	3
1.9	206	206	205	205	204	203	202	198	194	166	103	78	18	9	4
2.1	158	158	157	157	157	156	155	154	151	135	92	73	20	10	5
2.3	125	125	125	125	125	124	124	123	122	111	82	67	21	11	6
2.5	102	102	102	102	102	102	101	101	100	93	72	61	22	12	7
2.7	85	85	85	85	85	85	85	84	84	79	64	55	22	13	8
3.0	67	67	67	67	67	67	67	66	66	63	53	48	22	14	9

TABLE 7: Values of $K_{zz} \times 1000$ for uniform skin friction for $\mu=0.1$ and $L/a=120.0$
(+Tension, otherwise compression)

m \ n	0.0	0.02	0.04	0.06	0.08	0.1	0.12	0.16	0.2	0.4	0.8	1.0	2.0	2.5	3.0
0.1	0.0	1416	1216	965	733	547	409	235	144	26	4	2	0	0	0
0.3	0.0	560	551	535	514	489	461	401	342	141	28	14	1	0	0
0.5	0.0	459	456	451	444	435	425	400	371	220	61	32	2	1	0
0.7	0.0	589	584	575	563	548	531	493	452	268	87	50	4	2	1
0.9	0.0	1476	1391	1265	1129	1001	889	714	589	290	102	63	7	3	1
1.0	0.0	6127	3057	2032	1523	1219	1016	762	609	290	107	68	8	3	2
1.1	1745	1689	1546	1366	1189	1034	905	712	581	285	110	71	10	4	2
1.3	550	548	542	533	520	505	488	451	412	285	111	76	13	6	3
1.5	316	316	315	312	309	306	301	291	279	209	107	77	15	7	4
1.7	316	216	215	214	213	212	210	206	201	167	99	74	17	9	5
1.9	160	160	160	159	159	158	157	155	153	134	89	70	19	10	6
2.1	125	125	125	124	124	124	123	122	121	110	79	64	20	11	6
2.3	101	101	101	100	100	100	100	99	98	91	70	59	21	12	7
2.5	83	83	83	83	83	83	83	82	82	77	72	53	21	13	8
2.7	70	70	70	70	70	70	70	69	69	66	55	48	21	13	8
3.0	56	56	56	56	56	56	56	55	55	53	46	41	21	14	9

TABLE 8: Values of $K_{zz} \times 1000$ for uniform skin friction for $\mu = 0.3$ and $L/a = 120.0$ (+Tension, otherwise compression)

m \ n	0.0	0.02	0.04	0.06	0.08	0.1	0.12	0.16	0.2	0.4	0.8	1.0	2.0	2.5	3.0
0.1	0.0	3107	1260	981	740	550	409	235	144	26	4	2	0	0	0
0.3	0.0	3827	591	544	523	497	469	409	349	144	28	13	0	0	0
0.5	0.0	744	483	475	467	458	447	420	389	228	61	31	2	0	0
0.7	0.0	+2454	614	633	619	601	581	535	487	279	86	48	3	1	0
0.9	0.0	+360	1593	1450	1278	1120	984	776	632	301	102	61	6	2	1
1.0	0.0	7640	3299	2197	1642	1310	1089	812	645	301	106	66	7	3	1
1.1	1847	1793	1652	1469	1283	1117	976	765	620	297	110	70	9	3	2
1.3	599	597	590	580	566	549	530	488	445	269	112	75	12	5	2
1.5	343	343	342	339	336	332	327	315	301	222	110	77	14	7	3
1.7	233	233	232	232	230	229	227	222	216	178	102	76	17	8	4
1.9	172	172	172	171	171	170	169	167	164	143	93	72	18	9	5
2.1	134	134	133	133	133	132	132	131	129	116	82	67	20	11	6
2.3	107	107	107	107	107	107	105	105	104	96	73	61	21	12	7
2.5	88	88	88	88	88	88	88	87	86	81	64	55	21	13	7
2.7	74	74	74	74	74	74	74	73	73	69	57	50	21	13	8
3.0	59	59	59	59	59	59	58	58	58	56	48	43	21	14	9

TABLE 9: Values of $K_{zz} \times 1000$ for uniform skin friction for $\mu=0.5$ and $L/a=120.0$
(+Tension, otherwise compression)

m \ n	0.0	0.02	0.04	0.06	0.08	0.1	0.12	0.16	0.2	0.4	0.8	1.0	2.0	2.5	3.0
0.1	0.0	2228	1217	931	710	533	400	232	143	27	4	1	0	0	0
0.3	0.0	971	580	541	520	495	468	410	351	148	28	13	0	0	0
0.5	0.0	261	490	499	491	482	470	442	409	239	61	30	1	0	0
0.7	0.0	+77	662	697	682	662	639	587	532	297	86	46	2	0	0
0.9	0.0	888	1713	1605	1424	1251	1100	864	698	319	101	59	4	1	0
1.0	0.0	7289	3702	2472	1843	1466	1214	199	709	319	106	64	6	2	1
1.1	2464	2369	2132	1842	1566	1333	1145	875	697	318	110	69	7	2	1
1.3	730	727	718	703	684	661	634	578	520	298	116	75	10	4	2
1.5	407	407	405	401	397	391	385	369	351	251	116	79	13	5	2
1.7	272	272	271	270	268	266	264	258	250	201	110	79	15	7	3
1.9	198	198	198	197	196	195	194	191	188	161	100	76	17	8	4
2.1	152	152	152	152	151	151	150	149	146	131	90	71	19	10	5
2.3	121	121	121	121	121	120	120	119	118	108	80	65	20	11	6
2.5	99	99	99	99	99	99	98	98	97	91	70	60	21	12	7
2.7	83	83	83	83	83	82	82	82	81	77	72	54	21	13	8
3.0	65	65	65	65	65	65	65	64	64	61	52	46	21	13	8

TABLE 10 : Settlement Analysis for a Pile Group ($P_o = 25t$, $L = 12m$, $L/d = 30$)

Layer	Layer thickness $\delta = \triangle h/L$	Depth to mid-layer $m = z/L$	$K = \frac{\delta \times .4343 C_e}{1 \times e} = 0.0653$	Author's: Vertical stress coefficient K_{zz}: Pile 1 $n = .0236$	Pile 2 + Pile 3 $n = .0850$	Pile 4 $n = .1178$	ΣK_{zz}	$\frac{\triangle\sigma_1}{\sigma_1} = .0084 \times \frac{K_{zz}}{m}$	$\rho/L = K\, ln\left(1 + \frac{\triangle\sigma_1}{\sigma_1}\right)$
0-0.2L	0.2	0.1	0.013	2.236	1.568	0.456	4.260	0 3580	39.80×10^{-4}
0.2L-0.4L	0.2	0.3	0.013	1.100	1.112	0.471	2.683	0.0751	9.72
0.4L-0.6L	0.2	0.5	0.013	0.563	0.936	0.446	1.945	0.0326	4.17
0.6L-0.8L	0.2	0.7	0.013	0.790	1.312	0.579	2.681	0 0321	4.11
0.8L-0.9L	0.1	0.85	0.007	2.096	2.400	0.931	5.427	0.0536	3.40
0.9L-1.1L	0.2	1.0	0.013	6.928	3.480	1.220	11.628	0.0975	12.13
1.1L-1.5L	0.4	1.3	0.026	0.673	1.268	0.587	2.528	0.0163	4.16
1.5L-1.9L	0.4	1.7	0.026	0.251	0.496	0.244	0.991	0.0049	1.22
1.9L-2.3L	0.4	2.1	0.026	0.142	0.282	0.140	0.564	0.0023	0.60
2.3L-2.7L	0.4	2.5	0.026	0.088	0.186	0.092	0.366	0 0012	0.31
									79.62×10^{-4}